Calhoun
Institutional Archive of the Naval Postgraduate School

Calhoun: The NPS Institutional Archive
DSpace Repository

Theses and Dissertations
1. Thesis and Dissertation Collection, all items

1960

Gamma-gamma angular correlation in the decay of cobalt 60.

Verser, Fort A.

Monterey, California: U.S. Naval Postgraduate School

http://hdl.handle.net/10945/12250

Downloaded from NPS Archive: Calhoun

DUDLEY
KNOX
LIBRARY

Calhoun is the Naval Postgraduate School's public access digital repository for research materials and institutional publications created by the NPS community. Calhoun is named for Professor of Mathematics Guy K. Calhoun, NPS's first appointed -- and published -- scholarly author.

Dudley Knox Library / Naval Postgraduate School
411 Dyer Road / 1 University Circle
Monterey, California USA 93943

http://www.nps.edu/library

NPS ARCHIVE
1960
VERSER, F.

GAMMA-GAMMA ANGULAR CORRELATION IN THE DECAY OF COBALT 60

FORT A. VERSER, JR.

LIBRARY
U.S. NAVAL POSTGRADUATE SCHOOL
MONTEREY, CALIFORNIA

UNITED STATES
NAVAL POSTGRADUATE SCHOOL

THESIS

GAMMA-GAMMA ANGULAR CORRELATION
IN THE DECAY OF COBALT 60

by

Fort A. Verser, Jr.

12ND P2238 (1-59)

GAMMA-GAMMA ANGULAR CORRELATION IN THE DECAY OF COBALT 60

* * * * *

Fort A. Verser, Jr.

GAMMA-GAMMA ANGULAR CORRELATION
IN THE DECAY OF COBALT 60

by

Fort A. Verser, Jr.

Captain, United States Army

Submitted in partial fulfillment of
the requirements for the degree of

MASTER OF SCIENCE
IN
PHYSICS

United States Naval Postgraduate School
Monterey, California

1 9 6 0

PS ARCHIVE
160
ERSER, T

GAMMA-GAMMA ANGULAR CORRELATION
IN THE DECAY OF COBALT 60

by

Fort A. Verser, Jr.

This work is accepted as fulfilling
the thesis requirements for the degree of
MASTER OF SCIENCE
IN
PHYSICS
from the
United States Naval Postgraduate School

ABSTRACT

To further the program at the U. S. Naval Postgraduate School in the investigation of the properties of the low-lying excited states of nuclei, the equipment necessary to perform gamma-gamma directional angular correlation experiments was assembled and tested.

This thesis describes this equipment in considerable detail and the procedure followed in testing it using the well-known gamma cascade of Ni^{60}. The observed anisotropy agreed with the theoretical value within statistical expectations. However, the shape of the observed correlation function was distorted indicating an as yet unknown instrumental malfunction. Suggestions for improvements in the equipment are made.

The author wishes to express his appreciation for the assistance given him by Professor Harry E. Handler for initiating this work and for his guidance throughout this investigation. Appreciation is expressed to Professor Edmund A. Milne for valuable discussions on various aspects of this work. Professor William W. Hawes was generous in supplying some of the electronic equipment used in this investigation. The cooperation and assistance of Mr. Kenneth C. Smith and Mr. Robert C. Moeller were indispensable.

TABLE OF CONTENTS

CHAPTER PAGE

I. INTRODUCTION 1

II. THEORETICAL CONSIDERATIONS 3

III. DESCRIPTION OF EQUIPMENT 11

- A. Angular Correlation Table 13
- B. Detection of the Radiation 16
- C. Energy Selection 18
- D. Time Comparison 19
- E. Counting 20

IV. EXPERIMENTAL PROCEDURE 21

- A. Pulse Shaping 25
- B. Resolution of the Crystals 25
- C. Test of Scalers 26
- D. Check on Source Positioning 26
- E. Scattering 26
- F. Determination of Source Strength . . . 27
- G. Choice of Pulse Height Selection Limits 29
- H. Choice of Coincidence Resolving Times 30
- I. Reference Counting Rate 34
- J. Background Measurements 35
- K. Measurement of Scaler Resolving Times 35

CHAPTER PAGE

L. Measurement of Coincidence Resolving Time 36

M. Solid Angle Correction 38

N. Angular Correlation Runs 38

V. EXPERIMENTAL RESULTS 40

A. Coincidence Resolving Time 42

B. Angular Correlation Data 42

C. Experimental Angular Correlation Function 43

D. Experimental Anisotropies 44

VI. DISCUSSION OF RESULTS 46

A. Solid Angle Corrections 46

B. Comparison between Experiment and Theory 49

VII. CONCLUSIONS 53

LIST OF FIGURES

FIGURE PAGE

1. Angular Correlation Table 12

2. Electronic System 14

3. Schematic Diagram of Electronic System . . . 15

4. Gamma Ray Spectrum of Co^{60} 31

5. Illustrating Time Uncertainty due to Energy Selection 32

6. Comparison Between Experimental and Theoretical Correlation Functions 51

LIST OF TABLES

TABLE PAGE

1. Weighted Means of $\overline{W}'(\theta_i)$ 43
2. Least Square Coefficients 44
3. Solid Angle Correction Parameters 49

CHAPTER I

INTRODUCTION

The first paper on angular correlation of successive nuclear radiations in which the explicit theoretical correlation functions were derived was in 1940 by Hamilton [1]. It was apparent from the beginning that this was a very powerful means of investigating the low-lying excited states of nuclei. But successful experiments had to wait many years for advances in electronics to provide coincidence circuits of sufficiently short resolving time and for the improvement of radiation detection techniques. The first successful attempt to observe an angular correlation between two successively emitted gamma rays was in 1947 by Brady and Deutsch who used Geiger counters as detectors [2]. Really precise measurements of angular correlations involving gamma radiation had to wait until a means of detection more efficient and reliable than Geiger counters could be developed. Since in this work, we measure Poissonly-distributed variables, we are plagued by statistical fluctuations; hence for precision, a great number of quanta must be counted and under these conditions Geiger counters prove quite inadequate. With the development of the scintillation

crystal and photomultiplier tube, it became possible in a single day to measure a correlation to a precision that would have required many months to achieve using Geiger counters. The development of scintillation crystals of sodium-iodide activated by small amounts of thallium as an impurity also provided a means of measuring gamma-ray energies with high precision.

CHAPTER II

THEORETICAL CONSIDERATIONS

The study of the properties of low-lying excited nuclear states is greatly facilitated by a nuclear spectroscopic tool known as angular correlation or more completely "angular correlation of successive nuclear radiations". The short life-time of most excited nuclear states makes their investigation by direct means such as resonance methods next to impossible. Hence we must probe these states indirectly, and a method that comes immediately to mind in the case of low-lying states is the study of the radiations which preceed and succeed them.

The probability of emission of a particle or quantum by a radioactive nucleus depends in general on the angle between the nuclear spin axis and the direction of emission. Under ordinary circumstances, due to the random orientation of the nuclei in space, the radiation pattern can not be observed.

If, however, an ensemble of nuclei is preferentially oriented, a radiation pattern can be observed. One method of arriving at such an ensemble of nuclei consists in placing a radioactive sample in a strong magnetic field or

electric field gradient at a very low temperature, thereby orienting or aligning the nuclei, and then measuring the angular distribution of the emitted radiation with respect to the applied field.

Another method consists of selecting only those nuclear states whose spins happen to lie in preferred directions. This can be accomplished if a nucleus decays by the successive emission of two radiations, R_1 and R_2. Although the spin of the original nucleus may have an arbitrary orientation in space, the observation of R_1 in a fixed direction selects an ensemble of residual nuclear states whose angular momentum vectors are related to this direction. The succeeding radiation R_2 which is emitted by these states then has preferred angles of emission with respect to the direction of R_1.

When we investigate some property of these radiations as a function of the angle between their propagation vectors we do "angular correlation". As one can imagine, the field is very broad; however, it can be subdivided both as to the nature of the radiations involved and as to the particular property of the radiations under investigation. In the former case, the theory is broad enough to include any of the well-known nuclear emissions, such as beta rays, gamma

rays, alpha particles and neutrinos in any allowed combination. In the latter case, there are two general properties of the radiations which divide the field of angular correlation into (a) "directional correlation", wherein one measures the relative probability of emission of the second radiation as a function of the angle relative to the first, and (b) "polarization correlation", wherein one measures the relative probability of emission for two radiations, of a specified relative polarity, as a function of the included angle.

Since this work is concerned with the directional correlation of a gamma-gamma cascade, we will restrict ourselves to a discussion of the theory involved in this type of emission. In the following, references to "angular correlation", without qualifying phrases or adjectives, will be concerned with the direction-direction gamma-gamma cascade in which the radiations are emitted consecutively.

Consider an excited nucleus that emits in rapid succession two radiations, R_1 and R_2. In order that the correlation exhibit maximum anisotropy, the angular momentum vector of the intermediate state must not change direction before the second radiation R_2 is emitted. Stated another way, the mean life for the emission of the second radiation

must be short compared to the period of precession of the nuclear spin of the intermediate state, under the influence of possible spin-couplings. There are two types of spin-couplings to be considered: (1) the coupling of the intermediate state magnetic moment to a magnetic field and (2) the coupling of the quadrupole moment in the intermediate state to an electric field gradient. The presence of such spin-couplings will attenuate the correlation in the sense that it will be more isotropic than if due to undisturbed nuclei. Experimentally it is observed that the correlation can be wiped out entirely when the mean life of the intermediate state is of the order of the precession period. The precession period corresponding to these couplings is of the order of 10^{-8} seconds.

The principal information obtainable from an angular correlation measurement is the total angular momentum quantum numbers of the nuclear levels involved and the multipole order of the emitted radiations. To be more precise, it will yield the spins of the nuclear levels, but not the parities. If at least one of the transitions is not a pure multipole, it will also provide a means of obtaining the mixing ratio. Only in conjunction with other experiments is it possible to establish a complete decay scheme.

Today, angular correlation measurements are a well established tool in nuclear spectroscopy.

The fact that the angular correlation function $W(\theta)$ does not depend on the change in parities of the nuclear states can be understood classically. Electric and magnetic radiations of the same multipole order L are related by the transformation $E \longrightarrow H$, $H \longrightarrow -E$. This transformation leaves the Poynting vector and therefore the angular distribution of the radiation unaltered. It is thus impossible to distinguish between electric and magnetic radiation of the same multipole order by means of an angular correlation measurement.

The theoretical expressions for the correlation functions have been worked out for almost all cases of interest [3]. Let us consider a gamma-gamma cascade between states A, B, and C with spins I_a, I_b, and I_c respectively, in which both gamma rays, of multipole orders L_1 and L_2 respectively, are pure. Such a cascade will be denoted by $I_a(L_1)I_b(L_2)I_c$. The correlation function $W(\theta)$ is

$$W(\theta) = \sum_{n=0}^{n_{max}} A_n P_n(\cos\theta) = \sum_{n=0}^{n_{max}} B_n \cos^n \theta \qquad (1)$$

where P_n is the Legendre polynomial of even order n, and

[illegible]

[illegible]

$$[illegible]$$

[illegible]

n_{max} is the smallest even integer of the set of three numbers consisting of twice the spin of the intermediate state and twice the multipole order of each of the two gamma rays. The experimental investigation of a gamma-gamma cascade usually yields the three constants, A_0, A_2, and A_4 or B_0, B_2, and B_4. The constants depend on five parameters; the multipole orders L_1 and L_2 of the gamma rays and the spins I_a, I_b, and I_c of the nuclear states. Higher terms are generally not observed because the energies normally available in radioactive decays are such that multipoles with $L > 2$ possess half-lives $> 10^{-6}$ seconds. It is experimentally difficult or even impossible to measure the angular correlation function of a cascade involving an intermediate state with so long a half-life for the reasons previously enumerated. By comparing the experimentally determined constants with the theoretical constants, the spin numbers of the states and the multipole order of the radiations may be assigned. However, this assignment is not always unambiguous.

If we consider the gamma-gamma cascade between the three lowest states of the even-even nucleus, Ni^{60}, we find it expecially well suited for angular correlation measurements. Being an even-even nucleus, it has a spin of 0 in

its ground state and the second transition must therefore be pure. Only the first gamma ray can be mixed and this reduces considerably the number of possible interpretations of a measured correlation. Another consideration that makes Ni^{60} particularly well suited is the long lifetime of its parent nucleus Co^{60}.

A large number of publications [2, 4, 5, 6] contain data on Ni^{60} and this 4(2)2(2)0 cascade has become a "standard cascade" for testing angular correlation equipment. At one time there seemed to be a definite discrepancy between the expected theoretical correlation and experimental results. Later measurements, however, showed that the discrepancy was entirely due to improper treatment of the experimental data. The theoretical correlation function for the cascade in Ni^{60}, assuming point detectors, is

$$W(\theta) = 1 + 0.1020\, P_2(\cos\theta) + 0.0091\, P_4(\cos\theta) \qquad (2)$$

with an anisotropy

$$A = \frac{W(180^\circ) - W(90^\circ)}{W(90^\circ)} = 0.1667 \qquad (3)$$

As a part of a program at the U. S. Naval Postgraduate School on the investigation of low-lying excited states of

nuclei, the equipment necessary to perform a gamma-gamma directional angular correlation experiment was assembled. To check the reliability and performance of this equipment, the gamma-gamma angular correlation of the cascade of Ni^{60} was measured and compared with the theoretical function corrected for the finite size of the detectors.

CHAPTER III

DESCRIPTION OF EQUIPMENT

The equipment for a direction correlation experiment must provide a means for the detection and exclusion of radiation and for the recording of events. This necessitates the use of two channels, one to fix a direction in space, and the other to measure a relative angle.

The exclusion function of the apparatus is very broad. First of all it must exclude radiations proceeding at other than the selected angle. Second, it must exclude in each channel pulses arising from unwanted radiations of various energies. Third, it must compare the pulses in the two channels in time and exclude all of those which do not occur simultaneously or within a small time, τ, of one another.

Finally, the apparatus must record certain unexcluded, or selected events occuring during a given time interval and present them in a convenient manner. To accomplish these ends, the apparatus is divided into mechanical and electronic components.

Figure 1 is a photograph of the mechanical component of the equipment which consists of the angular correlation

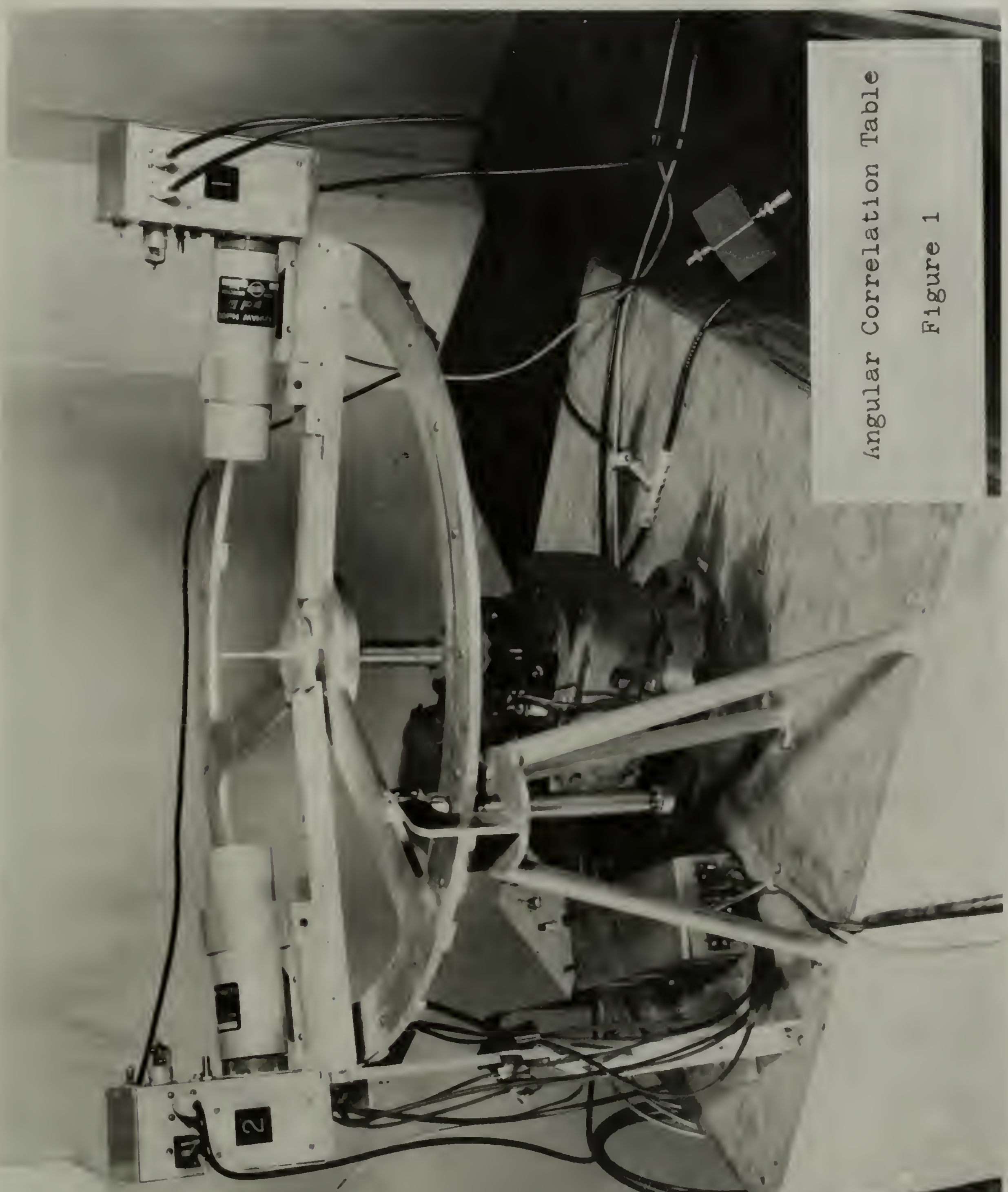

Angular Correlation Table

Figure 1

table.

The electronic system (Figure 2) has four primary tasks, viz., detection of the radiation, energy selection in each channel, time comparison between channels and counting. Detection was performed by the scintillation crystal and photomultiplier tube with their associated components and amplifiers. Energy selection was performed by the differential discriminators. Time comparison was performed in the coincidence analyzer and counting was done by Glo-tube scalers. Figure 3 is a schematic diagram of the electronic system.

A. Angular Correlation Table

The mechanical component consisted of the angular correlation table which provided a means of mounting the source and the detectors and measuring the angle between the fixed detector and a movable one. Centered on the table was the source container mount which consisted of an aluminum tube, of sufficient thickness to stop the beta particles from Co^{60}, with its axis perpendicular to the table and into which the source container could be inserted. The source container was made of lucite and had a volume that was 3/32 inch in diameter and 3/32 inch deep. After the source was placed in the container, a cover was sealed

table.

The electronic system (Figure 2) has four primary tasks, viz., detection of the radiation, energy selection in each channel, time comparison between channels and counting. Detection was performed by the scintillation crystal and photomultiplier tube with their associated components and amplifiers. Energy selection was performed by the differential discriminators. Time comparison was performed in the coincidence analyzer and counting was done by Glo-tube scalers. Figure 3 is a schematic diagram of the electronic system.

A. Angular Correlation Table

The mechanical component consisted of the angular correlation table which provided a means of mounting the source and the detectors and measuring the angle between the fixed detector and a movable one. Centered on the table was the source container mount which consisted of an aluminum tube, of sufficient thickness to stop the beta particles from Co^{60}, with its axis perpendicular to the table and into which the source container could be inserted. The source container was made of lucite and had a volume that was 3/32 inch in diameter and 3/32 inch deep. After the source was placed in the container, a cover was sealed

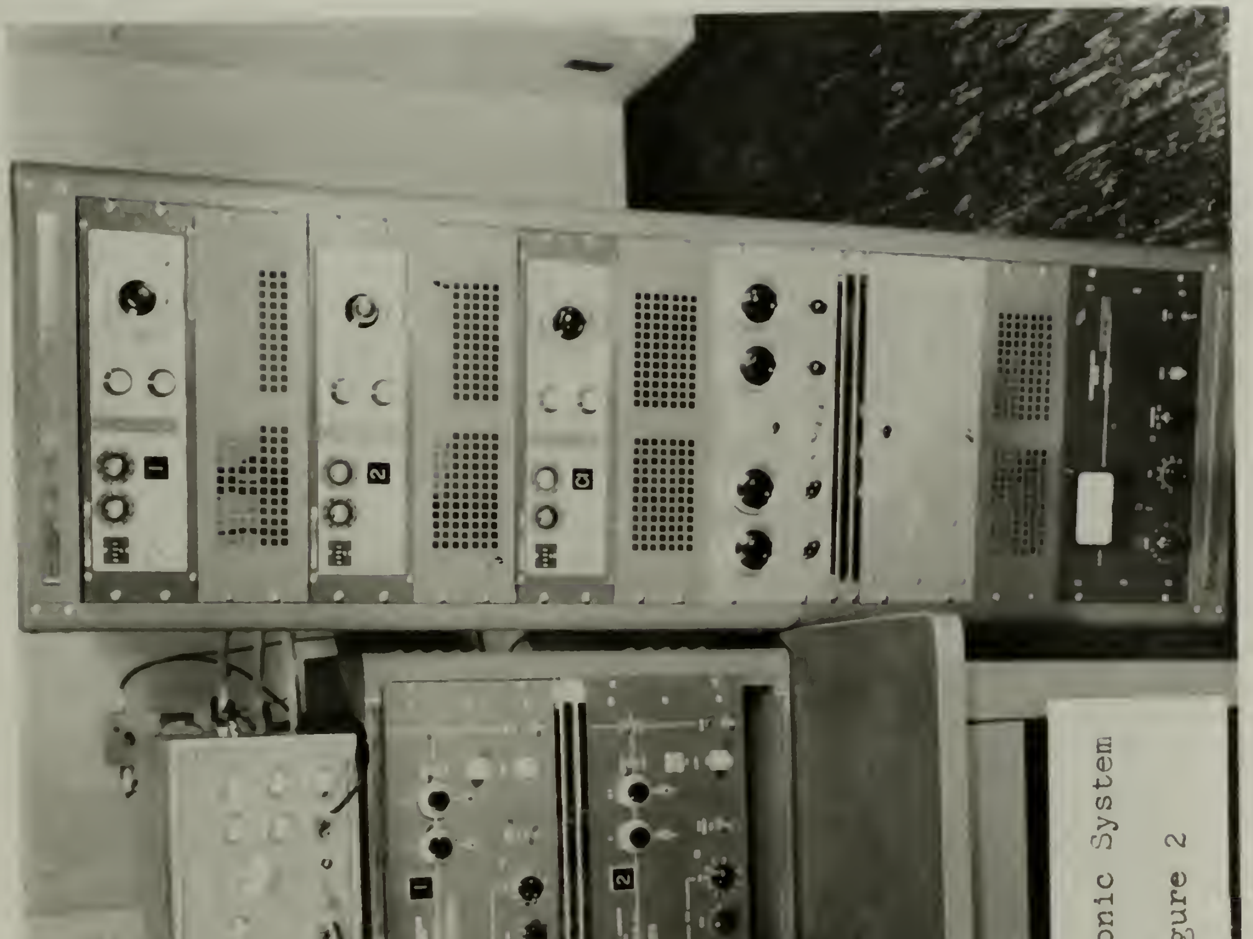

Electronic System

Figure 2

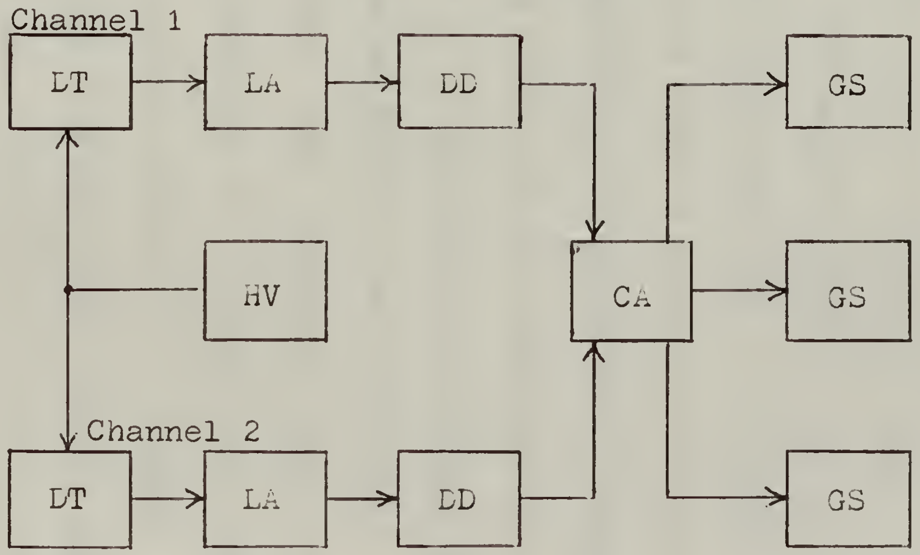

KEY:
DT-Detector
LA-Linear Amplifier
DD-Differential Discriminator
HV-High Voltage Power Supply
CA-Coincidence Analyzer
GS-Glo-Tube Scaler

Schematic Diagram of Electronic System

Figure 3

on it using an organic solvent. The detectors were mounted in a horizontal plane and radially with respect to the source volume. Provision was made for varying the distance between the source and the detectors. One detector was fixed while the second was movable and could be rotated through an angle of 180 degrees-from 90 degrees to 270 degrees. The movable detector was mounted on an aluminum "wheel" which was attached to a motor by way of a gear box. Provision was made so the field of the motor could be reversed permitting the table to be rotated in either direction. The table was also equipped with stops located at intervals of 15 degrees which enabled accurate positioning of the movable detector and provided a very rigid support for the table. The counting channels associated with each of these detectors will be denoted, henceforth, as Channel 1 for the movable detector and Channel 2 for the fixed detector. When the detectors were secured in their mounts, their axes were coplanar and intersected at the source volume. The detectors were positioned radially so they subtended a solid angle of approximately 1/16 steradian.

B. Detection of the Radiation

The gamma radiations were detected by Harshaw Integral Line scintillation detectors, Type 8S8/2. Each detector

consisted of a thallium-activated, cylindrical, sodium-iodide crystal, two inches in diameter and two inches thick, directly attached to an RCA 6342 photomultiplier tube with a rigid, high-index, optical coupling medium. The crystal and matching phototube were hermetically encapsulated in a low-mass, light-tight housing having a 0.015 inch aluminum entrance window. The container extended entirely over the base of the phototube, thus making the complete detector a plug-in unit. An internal magnetic shield consisting of one turn of 0.004 inch conetic AA foil, sufficient for the earths field, was included in the assembly. A 6AK5 cathode follower was mounted as an integral part of each detector. The phototubes were operated at approximately 76 volts per dynode.

The high voltage for the detectors was 1120 volts with a positive polarity and was supplied by a Hamner high voltage power supply, Model N-401. The output from the N-401 was split and sent to each detector. No provision was made for independently adjusting the high voltage of each detector. The N-401 provides continuously variable voltages from 500 to 1800 volts, positive or negative, and with a stability against line voltage changes of three parts per million per volt for line voltages from 105 to 125 volts

and for 1000 volts output.

The negative pulses from each photomultiplier tube were fed into a Hamner non-overload amplifier and pulse height discriminator, Model N-302. The Model N-302 consists of a non-overload pulse amplifier with power supply and a differential pulse height analyzer. The amplifier employs longtailed-pair fed-back loops. It provides a maximum gain of 10,000 with one-microsecond delay-line clipping at the input. The output is a positive pulse with a rise time less than 0.2 microseconds, a maximum amplitude of 120 volts and a width of approximately 1.7 microseconds.

C. Energy Selection

The positive pulse from the linear amplifier was fed into the differential discriminator which employs the well-known circuit consisting of two Schmitt trigger circuits feeding into an anti-coincidence circuit. Briefly, the operation is as follows. If an incoming positive pulse exceeds the potential setting of the dial which changes the lower discrimination level, the lower pulse height selector circuit fires and a pulse is produced and sent to the anti-coincidence circuit. If this incoming positive pulse does not exceed the potential selected by the setting of the dial which controls the width of the window, the upper

pulse height selector circuit does not fire and the pulse from the lower pulse height circuit passes through the anti-coincidence circuit. If on the other hand, the incoming pulse exceeds the width of the window, the upper pulse height selector circuit fires and a pulse is produced and sent to the anti-coincidence circuit which prevents either pulse from passing through this circuit.

D. Time Comparison

The output from each differential discriminator was fed into an Atomic Instrument Company, Model 502A, Coincidence Analyzer. The function of the coincidence analyzer was to select a pair of pulses, one from each channel, which occur within a preset time of one another. This time is called the resolving time and is represented by τ. The times of occurrence of the two events are sharply defined by using their voltage pulses to produce narrow pulses in the coincidence analyzer and then mixing these narrow pulses to detect the presence of coincidence counts. An integral pulse height discriminator is provided at each channel input to eliminate low amplitude noise pulses such as commonly occur in many preamplifiers or high gain pulse amplifiers. The nominal resolving time of each channel was set as desired by means of a selector switch located on the front

panel. This switch provides a choice of nominal resolving times of 1/4, 1/2, 1, or 2 microseconds. The output pulses were positive with at least 20 volts amplitude and a rise time of approximately 0.25-microseconds. The coincidence analyzer provides three outputs; the total pulses in Channel 1, the total pulses in Channel 2, and the coincidences between Channel 1 and Channel 2.

E. Counting

The outputs from the coincidence analyzer were fed into a bank of three Glo-tube scalers, each of which was capable of registering one million counts. One of these was used to count the total counts in Channel 1, another the total counts in Channel 2, and the third counted the total number of coincidences. Each scaler had an integral pulse height discriminator that was set to eliminate any low amplitude spurious counts from the coincidence analyzer.

CHAPTER IV

EXPERIMENTAL PROCEDURE

To perform an angular correlation measurement, the equipment must be capable of measuring the number of total coincidences as a function of the angle between the propagation vectors of the two radiations involved. The number of total coincidences is given by

$$C_t = C_g + C_a + C_b \tag{4}$$

where

C_t = the number of total coincidences

C_g = the number of coincidences due to the two radiations in cascade

C_a = the number of accidental coincidences due to the finite resolving time

C_b = the number of background coincidences

When the half-life of the source is long compared to the time required for the correlation measurements, Equation (4) can be rearranged and rewritten in terms of the counting rates.

$$\dot{C}_g = \dot{C}_t - \dot{C}_a - \dot{C}_b \tag{5}$$

$\dot{C}_g$ can also be expressed as a function of other variables:

$$\dot{C}_g = (\varepsilon_{11}\alpha_{11}\rho_{11}\varepsilon_{22}\alpha_{22}\rho_{22} + \varepsilon_{12}\alpha_{12}\rho_{12}\varepsilon_{21}\alpha_{21}\rho_{21})\Omega_1\Omega_2\phi_{12}\dot{N}_0\overline{W}(\theta_i) \quad (6)$$

where

$\dot{N}_0$ = the absolute source strength

ϕ_{jk} = the fraction of nuclei decaying by the emission of gamma ray "j" and gamma ray "k" in a cascade

Ω_i = the fractional solid angle subtended by the crystal in Channel "i"

ρ_{ij} = the fraction of gamma rays "j" which leave the source in the right direction to enter crystal "i" that are not absorbed before reaching the crystal

ε_{ij} = the total efficiency of the crystal in Channel "i" for gamma ray "j"

α_{ij} = the fraction of the number of gamma rays "j" captured by the crystal in Channel "i" whose pulse heights are accepted by the energy discrimination of Channel "i"

$\overline{W}(\theta_i)$ = the angular correlation function at an angle θ averaged over the solid angles used

We can find an expression for $\dot{N}_i$, the counting rate in Channel "i" in terms of the same variables.

$$\dot{N}_i = \Omega_i \phi_i \dot{N}_o \sum_j \varepsilon_{ij} \alpha_{ij} e_{ij} + \dot{N}_{ib} \tag{7}$$

where

ϕ_i = the number of gamma rays "i" produced per nucleus decaying

$\dot{N}_{ib}$ = the background counting rate in Channel "i"

Solving Equation (6) for the correlation function, we get

$$\overline{W}(\theta_i) = \frac{\dot{C}_g}{f\ \dot{N}_o} = \frac{\dot{C}_t - \dot{C}_a - \dot{C}_b}{f\ \dot{N}_o} \tag{8}$$

where f is the appropriate function of the ε's, α's, e's, Ω's, and ϕ_{12}.

Solving Equation (7) for $\dot{N}_o$

$$\dot{N}_o = \frac{\dot{N}_i - \dot{N}_{ib}}{p_i} \tag{9}$$

where p_i is the appropriate function of the ε's, α's, e's, Ω's, and ϕ's.

If we now multiply Equation (8) by $\frac{\dot{N}_o}{\dot{N}_o}$ and substitute Equation (9) for the $\dot{N}_o$'s that appear in the denominator,

we will get

$$\overline{W}(\theta_i) = \frac{(\dot{C}_t - \dot{C}_a - \dot{C}_b)\,\dot{N}_o\, g}{(\dot{N}_1 - \dot{N}_{1b})(\dot{N}_2 - \dot{N}_{2b})} \qquad (10)$$

where

$$g = \frac{p_1 p_2}{f}$$

Expressing g in terms of its variables,

$$g = \frac{(\varepsilon_{11}\alpha_{11}\rho_{11} + \varepsilon_{12}\alpha_{12}\rho_{12})(\varepsilon_{21}\alpha_{21}\rho_{21} + \varepsilon_{22}\alpha_{22}\rho_{22})\,\Omega_1\Omega_2\phi_1\phi_2}{(\varepsilon_{11}\alpha_{11}\rho_{11}\varepsilon_{22}\alpha_{22}\rho_{22} + \varepsilon_{12}\alpha_{12}\rho_{12}\varepsilon_{21}\alpha_{21}\rho_{21})\,\Omega_1\Omega_2\phi_{12}} \qquad (11)$$

Examination of this ratio will show that even though the numerator and denominator are sensitive to small gain fluctuations, the ratio is relatively insensitive. As we calculate the correlation function for various angles, g will also be insensitive to small eccentricities in the source. Therefore, the division of $\dot{C}_g$ by $\dot{N}_1\dot{N}_2$ gives a first order correction for small gain drifts and small errors in the positioning of the source.

The dependence of the coincidence rate on the position of the movable detector corresponds to the theoretical correlation function only under the assumption of a centered point source, point detectors, no scattering, and stability

of the electronic equipment. In order to compare experimental and theoretical results, the data must be corrected for the various deviations from the ideal arrangement. The correction for small gain drifts and small eccentricities in the source position was discussed in the previous paragraph. The method of correcting the data for the various deviations from the ideal arrangement will be discussed in the following paragraphs.

A. Pulse Shaping

To perform some of the operational checks, a laboratory double pulse generator was employed. The preamplifiers were modified by installing a switch which enabled a test pulse to be introduced into the electronic system in lieu of the pulse from the photomultiplier tube. Using various combinations of condensers and resistors, the output from the pulse generator was shaped to duplicate the output pulse of the scintillation crystal and photomultiplier tube.

B. Resolution of the Crystals

Using a Cs^{137} source, the resolution of the detectors was determined by standard methods. It was found that the resolution for Channel 1 was 12.1% while Channel 2 had a resolution of 11.2% for the full-energy peak of the Cs^{137}

0.662-Mev gamma ray.

C. Test of Scalers

To determine if all pulses were passing through the coincidence analyzer and counted by the scalers, a pulse of 10 volts amplitude was split and fed into Channel 1 and Channel 2 of the coincidence analyzer. The integral pulse discriminators at the input of the coincidence analyzer were each set at five volts. The total counts in Channel 1, Channel 2, and the coincidence output were recorded. It was found that the scalers counted together accurately to within plus or minus 0.002%.

D. Check on Source Positioning

As a test of the positioning of the source in the center of the correlation table and the effect of any external fields on the counting rate, the integral counting rate of a portion of the Co^{60} spectrum was measured in each channel as a function of the angle between the counters. Within statistical expectation, the counting rates were constant.

E. Scattering

Compton scattering occurring outside the detectors can give rise to unwanted coincidences. These in general

will tend to smear out the measured correlation function. This problem was minimized by the use of scintillation crystals as detectors and accepting only the full-energy peaks of the desired gamma rays.

F. Determination of Source Strength

If we assume a negligible background counting rate, Equation (5) becomes

$$\dot{C}_g = \dot{C}_t - \dot{C}_a$$

The statistical uncertainty in the result of a counting experiment can be calculated from the general principle that the uncertainty in counting a total of "n" particles is $\sqrt{n}$. For a total counting time T, the total number of coincidences is $\dot{C}_t T$ and the standard deviation in the total coincidence rate is

$$\sigma_t = \sqrt{\frac{\dot{C}_t}{T}} \qquad (12)$$

Then the standard deviation in the genuine coincidence rate is

$$\sigma_g^2 = \sigma_t^2 + \sigma_a^2 = \frac{\dot{C}_t}{T} + \frac{\dot{C}_a}{T}$$

and the fractional statistical error in the genuine coincidence rate is given by

$$\frac{\sigma_g}{\dot{C}_g} = \frac{1}{\sqrt{T}} \sqrt{\frac{\dot{C}_t + \dot{C}_a}{\dot{C}_t - \dot{C}_a}}$$

Therefore, in order to obtain the smallest fractional statistical error in the genuine coincidence rate, the quantities T and $\dot{C}_t - \dot{C}_a$ should be made as large as possible. For a fixed counting time, we would make $\dot{C}_a$ as small as possible. The accidental coincidence rate is given by

$$\dot{C}_a = 2\tau \dot{N}_1 \dot{N}_2 \simeq 2\tau \dot{N}_o^{\,2} \tag{13}$$

From Equation (6), the genuine coincidence rate is proportional to the absolute source strength. The ratio of genuine to accidental coincidences will therefore be

$$\frac{\dot{C}_g}{\dot{C}_a} \simeq \frac{1}{2\tau \dot{N}_o} \tag{14}$$

From Equation (13), we observe that we can reduce the accidental coincidence rate by either decreasing the resolving time or decreasing the absolute source strength. Therefore, for a given τ, as determined by the electronic system, the source strength must be kept as small as possible. However,

as the size of the source is decreased, the counting time must be increased to get a specified precision in the total coincidence rate. Thus a compromise must be reached between the precision attainable with the available circuitry and the time spent for counting.

The nominal minimum resolving time obtainable with the electronic system used in this experiment was approximately 0.25-microseconds. The approximate strength of the source used in this experiment was 0.05 millicuries of Co^{60} which was a water solution of $CoCl_2$ that just filled the source volume. This source gave a ratio of genuine coincidence rate to accidental coincidence rate of approximately 1.2.

G. Choice of Pulse Height Selection Limits

Since gamma rays from Compton scattering occurring outside the detectors can produce coincidences which will tend to smear out the correlation function, it is advantageous to use just the full-energy peaks of the gamma rays. For this reason, the discriminator settings in Channel 1 and Channel 2 were each chosen so they would accept only those pulses corresponding to the full-energy peaks of both gamma rays. The discriminator settings were determined by using the Co^{60} source and the double pulse generator. With the Co^{60} source in position, the gain of each linear

amplifier was adjusted so that the maximum amplitude of the pulses was of a convenient height. The positions of the full-energy peaks in each channel were then determined visually using the scale of the oscilloscope. The switches on the preamplifiers were then changed so pulses with independently adjustable amplitudes from the double pulse generator could be introduced into each electronic channel. Using the gain control on the pulse generator, each pulse was adjusted to an amplitude corresponding to E_1 (Figure 4). With the pulses thus set, the dial on each differential discriminator which positions the lower discrimination level was adjusted so each channel was just registering full counts. Each pulse was then adjusted to an amplitude corresponding to E_2 and the dial on each differential discriminator which controls the width of the window was adjusted so each channel was again just registering full counts. With these settings on the differential discriminators, only those pulses corresponding to the full-energy peaks would be passed to the coincidence analyzer by each channel.

H. Choice of Coincidence Resolving Times

The limitation on the minimum resolving time can best be understood by referring to Figure 5. It is based on the

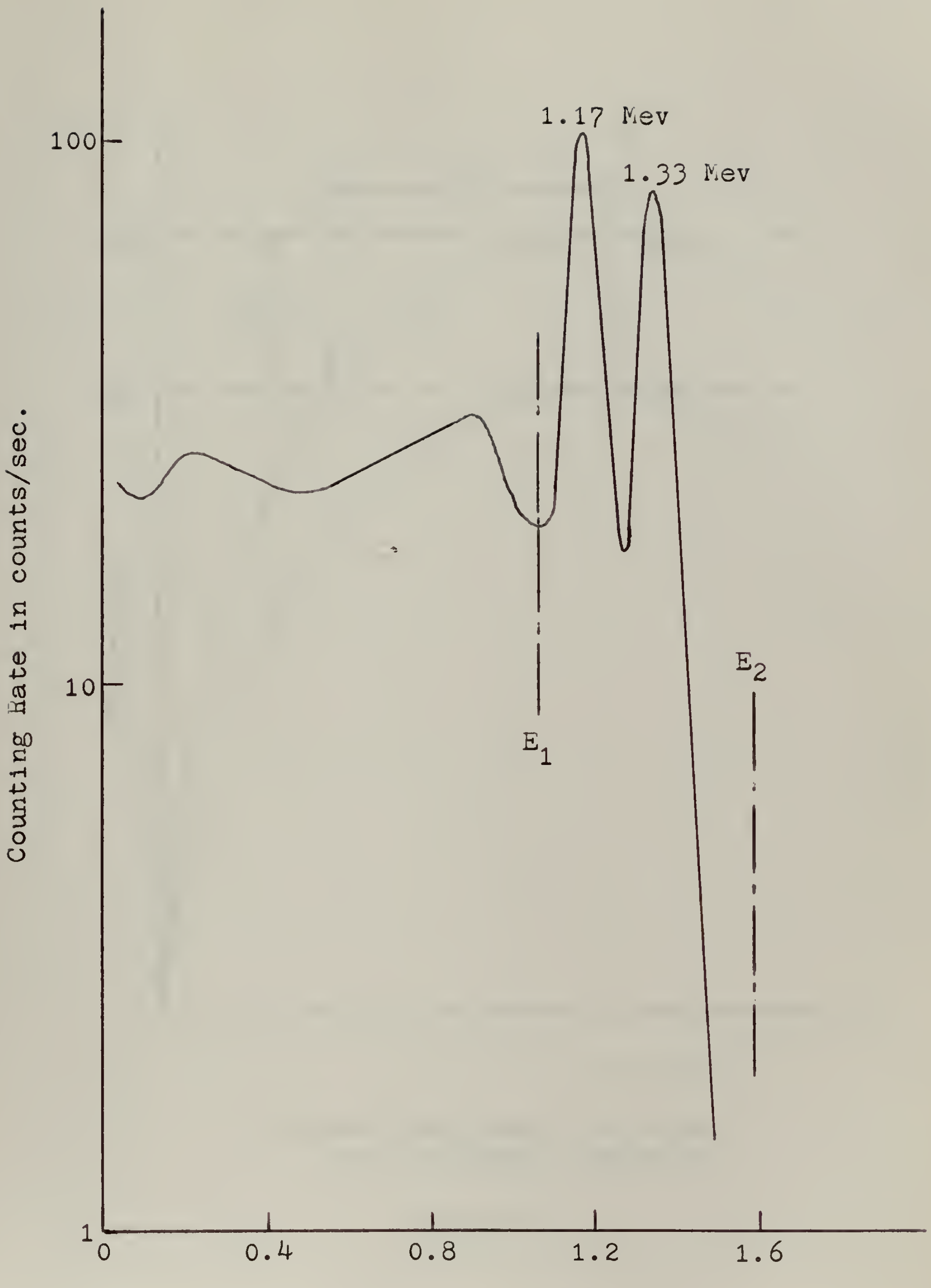

Gamma Ray Spectrum of Co^{60}

Figure 4

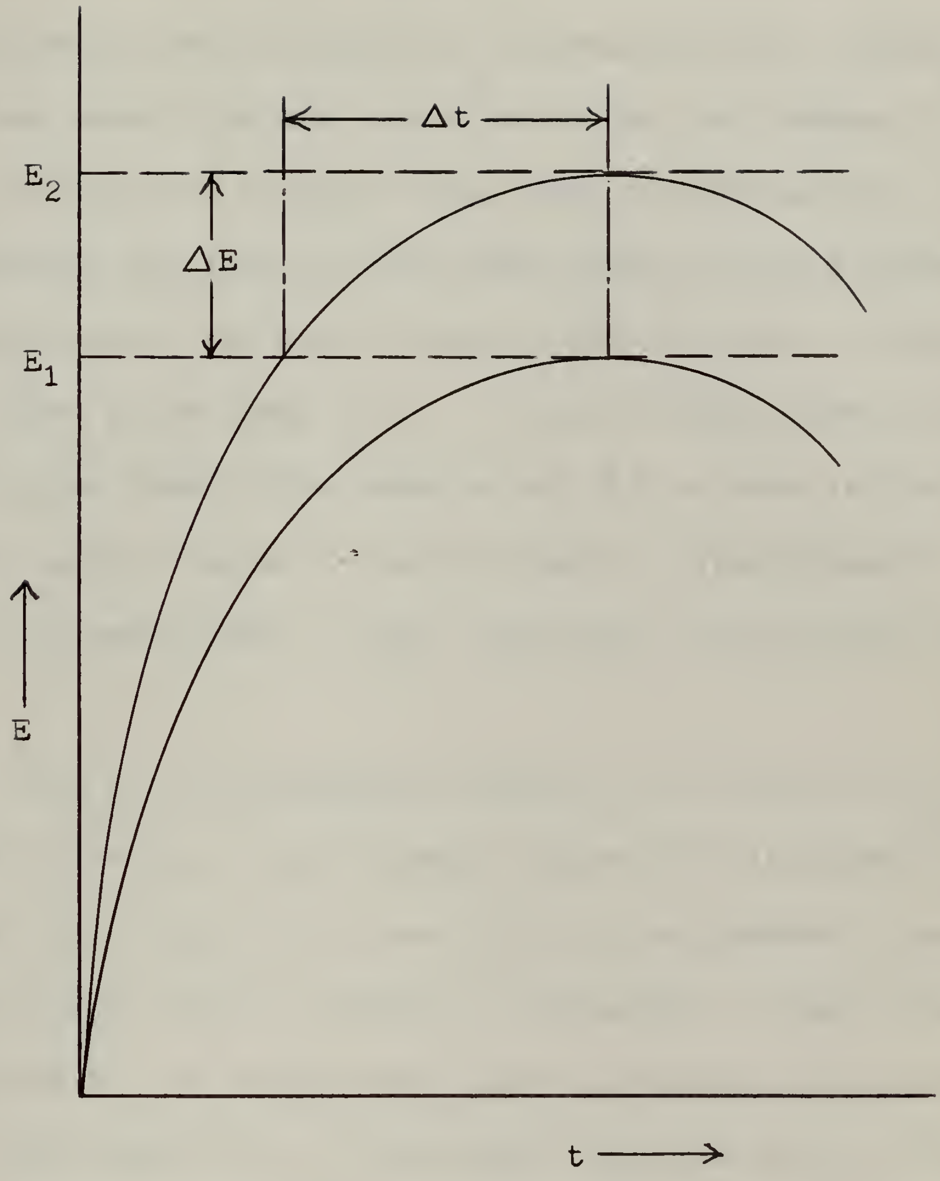

Illustrating Time Uncertainty
Due to Energy Selection

Figure 5

principle of operation of the differential discriminators which was previously discussed. The only pulses which will pass through the differential discriminator in either channel are those from the linear amplifier in a range, E_1 to E_2. The time of firing of the lower discrimination level determines the time of the output pulse of the differential discriminator, and this circuit fires when the voltage of the input pulse rises to E_1. It can be seen directly from the figure that a time uncertainty $\triangle t$ is thus introduced in the output pulse of the differential discriminator. One is thus constrained to use a resolving time greater than $\triangle t$.

With all the equipment adjusted as it would be for the correlation runs, simultaneous pulses with independently adjustable heights from the double pulse generator were fed into each electronic channel. The height of each pulse was adjusted so the channel was just registering full counts. The time separation of the output pulses from the differential discriminators was measured using the oscilloscope. This procedure was repeated for pulses of all amplitudes in $\triangle E$ of Channel 1 and pulses of all amplitudes in $\triangle E$ of Channel 2. The oscilloscope measurements gave the maximum time separation between the pulses being fed into the

coincidence analyzer. This permitted the choice of a nominal resolving time. This nominal resolving time was set on the resolving time switches of each channel of the coincidence analyzer and the coincidence counting rate was checked against each single channel rate as a function of the pulse height. This verified that all legitimate coincidences were counted.

I. Reference Counting Rate

With the discriminator in each channel adjusted as above, the integral counting rate of the Co^{60} spectrum in each channel was determined. This gave a reference counting rate for each channel. During the course of the correlation runs, the discriminator settings or the gains of the linear amplifiers were adjusted before each run so that the integral counting rate agreed closely with these reference rates.

As a measure of the gain fluctuations during each counting run, the integral counting rate of each channel was measured after each counting run using the same discriminator settings that were employed during the run. The maximum variation between this counting rate and the reference counting rate for each channel was two per cent for

any actual correlation run.

J. Background Measurements

With the discriminators at the same settings as were used during the correlation runs, background runs were made before and after the correlation runs. The background coincidence counting rate was negligible and the background counting rate of each channel was approximately 0.3 per cent of the gross counting rates during the correlation runs. These background rates were applied as corrections to the gross counting rates obtained during the correlation runs.

K. Measurement of Scaler Resolving Times

To correct the total counts in each channel for losses in the counting circuits, it was necessary to determine the scaler resolving times. Since the scaling losses were small, the precision in the measurement of the resolving times did not have to be better than 10 per cent. The scaler resolving times were determined by two methods; (1) using a laboratory double pulse generator and an oscilloscope and (2) by the two source method.

Two pulses from the double pulse generator were introduced into the channel under test. The pulses had a repeti-

tion rate of 1000 per second and a variable time separation. The separation between the two pulses was then reduced until the scaler began to miss counts and the pulse separation was then measured directly on the oscilloscope. Using this method, the resolving times of the scalers were determined to be approximately three microseconds.

The resolving times were also determined by the two source method. The resolving times determined by this method and subsequently used in the calculations were 3.51 ± 0.12 microseconds for Channel 1 and 4.65 ± 0.13 microseconds for Channel 2. Since the coincidence counting rate was very low, it was not necessary to determine the resolving time of the coincidence scaler.

L. Measurement of Coincidence Resolving Time

To calculate the number of accidental coincidences occurring in the total coincidence channel, a knowledge of the coincidence resolving time is necessary. The accidental coincidence rate, which frequently constitutes a large part of the total coincidence counting rate, is given by Equation (13).

The Co^{60} source was placed in position on the angular correlation table and an 0.8 microsecond delay line was inserted into Channel 2, between the differential discrim-

inator and the coincidence analyzer, to eliminate any genuine coincidences. The accidental counting rate and the counting rate of each channel were measured and 2τ was calculated using Equation (13). It was found that the coincidence resolving time was a function of the counting rate. This was due to the electronic circuits of the coincidence analyzer used. As the counting rate increased above 1,600 per second, the resolving time decreased. Therefore, it was necessary to decide on the counting rates that were to be used during the correlation runs and determine the resolving time for these rates. This was possible because Co^{60} has a relatively long half-life and consequently a steady counting rate. This particular coincidence analyzer would be unsuited for correlation experiments on materials that do not provide a steady counting rate. The resolving time was determined at the beginning of the correlation runs and again half-way through. The results of these determinations are:

$$\tau = 0.2057 \pm 0.0019 \text{ microseconds}$$

$$\tau = 0.2066 \pm 0.0018 \text{ microseconds}$$

The consistency of these values gave a dependable check on the stability of the electronic equipment.

M. Solid Angle Correction

The method of correcting the theoretical correlation function for a finite detector will be discussed in Section A, Chapter VI.

N. Angular Correlation Runs

Since the angular correlation table was equipped with stops located at intervals of 15 degrees, it was initially decided to make six two-hour runs at each position with the movable detector located at 90°, 105°, 120°, 135°, 150°, 165°, and 180°. To minimize any systematic fluctuations in the equipment, the angular order in which they were taken was varied. Before each run, the integral counting rate of each channel was adjusted to agree with the reference counting rate. The single channel counting rates were approximately 1400 counts per second. Each run yielded a total coincidence rate of approximately 1.5 counts per second of which about 45 per cent were accidentals.

To improve the statistics, six more runs of two-hours each were taken with the movable detector positioned at 90° and 180°. One run of a 12-hour counting period was also taken at each of the seven angles interspersed between the two-hour runs.

The two-hour runs for a given angle were checked for statistical consistency by the use of the chi-square distribution test and all but one run at one angle were statistically acceptable. Another two-hour run was made to replace this one. The result of the twelve-hour run at each angle was compared with the mean of six of the two-hour runs at that angle by using the t-distribution test. The data for the twelve-hour periods was not consistent in all cases and therefore it was decided to discard these data as being unreliable. It is believed that the inconsistency was due to the occurrence of large gain fluctuations during the twelve-hour counting periods.

CHAPTER V

EXPERIMENTAL RESULTS

The correlation function for each run, $\overline{W}(\theta_i)$, is given by

$$\overline{W}(\theta_i) = \frac{g\,\dot{N}_o}{(\dot{N}_1 - \dot{N}_{1b})(\dot{N}_2 - \dot{N}_{2b})}(\dot{C}_t - \dot{C}_a - \dot{C}_b)$$

Since g and $\dot{N}_o$ were constant for this experiment, it was sufficient to calculate a modified correlation function given by

$$\overline{W}'(\theta_i) = \frac{\overline{W}(\theta_i)}{g\,\dot{N}_o} = \frac{\dot{C}_t - \dot{C}_a - \dot{C}_b}{(\dot{N}_1 - \dot{N}_{1b})(\dot{N}_2 - \dot{N}_{2b})} \qquad (15)$$

This necessitates the determination of seven counting rates.

The standard deviation of any observed counting rate, $\dot{X}_i$, is given by

$$\sigma_i = \sqrt{\frac{\dot{X}_i}{T_i}}$$

where

T_i = the counting time for determining X_i events

To determine the weighted mean of a series of measurements, the inverse square of the standard deviation of each

measurement was used as a weighting factor.

$$\bar{\dot{X}} = \frac{\sum \frac{\dot{X}_i}{\sigma_i^2}}{\sum \frac{1}{\sigma_i^2}} \tag{16}$$

The standard deviation of the weighted mean was calculated from the standard deviations of the individual measurements.

$$\frac{1}{\sigma^2(\bar{X})} = \sum \frac{1}{\sigma_i^2} \tag{17}$$

The single-channel counting rates and the background counting rates, $\dot{N}_{1b}$ and $\dot{N}_{2b}$, for each run were experimentally determined. Correcting the single-channel counting rates for scaling losses gave $\dot{N}_1$ and $\dot{N}_2$.

The accidental counting rate for each run was calculated from Equation (13) using the weighted mean of the experimentally determined coincidence resolving times.

The total coincidence counting rate, $\dot{C}_t$, for each run was experimentally determined. The background coincidence rate, $\dot{C}_b$, was negligible throughout the experiment.

Each $\overline{W}'(\theta_i)$ and its standard deviation were calculated and the weighted means and their standard deviations were

computed for each angle.

Using the method of least squares, the weighted means of the experimental correlation functions were fitted to each of the two functional forms of the theoretical correlation function as given by Equation (1). The standard deviations of the least square coefficients were also calculated.

These calculations together with the results are given in the following sections.

A. Coincidence Resolving Time

Using the coincidence resolving times as determined in Section E, Chapter IV, the weighted mean of the resolving time and its standard deviation were calculated using Equations (16) and (17). The result of this calculation is given below.

$$\tau = 0.20694 \pm 0.00096 \text{ microseconds}$$

B. Angular Correlation Data

The accidental coincidence rate was calculated for each correlation run using Equation (13). The background coincidence rate was zero. The correlation function, $\overline{W}'(\theta_i)$, was then calculated using Equation (15) and its standard deviation was determined principally from those

of $\dot{C}_t$ and $\dot{C}_a$.

The weighted mean of the runs at each angle and its standard deviation were computed. These results are tabulated in Table 1.

Table 1

Weighted Means of $\overline{W}'(\theta_i)$

θ (degrees)	Weighted Mean	σ
90	4795	30
105	4770	42
120	4778	42
135	4996	42
150	5313	43
165	5521	44
180	5562	31

C. Experimental Angular Correlation Function

The theoretical correlation function as defined by Equation (1) is a finite series of even-ordered Legendre Polynomials or of even-powered cosine functions (see Chapter II). Each of these functions was fitted to the weighted

[illegible]

[illegible]

[illegible]

[illegible]

[illegible]	[illegible]	[illegible]
[illegible]	[illegible]	[illegible]
[illegible]	[illegible]	[illegible]
[illegible]	[illegible]	[illegible]
[illegible]	[illegible]	[illegible]
[illegible]	[illegible]	[illegible]
[illegible]	[illegible]	[illegible]

[illegible]

[illegible]

means of the experimental correlation functions given in Table 1 by the method of least squares [7] and the experimental values and their standard deviations for the coefficients A_n and B_n were found. These values, normalized so that $A_o = B_o = 1$, are listed in Table 2.

Table 2

Least Square Coefficients

A_o	A_2	A_4
1.0000 ± 0.0034	0.0961 ± 0.0055	0.0339 ± 0.0071

B_o	B_2	B_4
1.0000 ± 0.0054	0.0176 ± 0.0327	0.1537 ± 0.0319

D. Experimental Anisotropies

The anisotropy is defined:

$$\bar{R} = \frac{\bar{W}(180^{o}) - \bar{W}(90^{o})}{\bar{W}(90^{o})}$$

The anisotropies for the two least-square curves were calculated from the experimental correlation functions. These

[illegible]

[illegible]

[illegible]

[illegible]

[illegible]

[illegible]

values are

$$\overline{K}(P_n) = 0.172$$

$$\overline{K}(\cos^n \epsilon) = 0.171 \pm 0.027$$

The standard deviation for the latter was calculated by a formula presented by Klema and McGowan [6].

CHAPTER VI

DISCUSSION OF RESULTS

To determine the validity of the results it is necessary to compare the experimental and the theoretical correlation functions. Since the theoretical correlation function, $\overline{W}(\theta)$, as derived by Hamilton [1], is based upon the assumption of point detectors, a correction must be made for the solid angles of the detectors. A comparison between the experimental and the corrected theoretical correlation functions will give an indication as to whether or not the equipment is functioning properly.

The method of correcting for the solid angle of the detectors and a comparison between the experimental and the theoretical correlation functions will be discussed in the following sections.

A. Solid Angle Corrections

The solid angle correction which must be applied to the theoretical correlation function to enable a comparison to be made with the measured one is described by Rose [7]. The correction involves the numerical evaluation of integrals of the form

$$I_{n,i} = \int_0^{\gamma_i} P_n(\cos \phi)\left(1 - e^{-T_i X_i(\phi)}\right) \sin \phi \, d\phi \qquad (18)$$

where

T_i = the full-energy absorption coefficient of the detector in Channel "i" for the gamma ray of interest

γ_i = the half-angle subtended by the front face of the crystal in Channel "i"

and

$$X_i(\phi) = t_i \sec \phi \qquad \text{for} \qquad 0 \leq \phi \leq \tan^{-1}\frac{r_i}{h_i + t_i}$$

$$X_i(\phi) = r_i \csc \phi - h_i \sec \phi \qquad \text{for} \qquad \tan^{-1}\frac{r_i}{h_i + t_i} \leq \phi \leq \gamma_i$$

where

h_i = the distance from the source to the crystal in Channel "i"

t_i = the thickness of the crystal in Channel "i"

r_i = the radius of the crystal in Channel "i"

The attenuation factors, Q_n, are expressed as the product of two attenuation coefficients:

$$Q_n = \left[\frac{I_{n,1}}{I_{0,1}}\right]\left[\frac{I_{n,2}}{I_{0,2}}\right] \qquad (19)$$

and the corrected theoretical correlation function is

$$\overline{W}(\theta) = \sum_{n=0}^{n_{max}} Q_n A_n P_n(\cos\theta) = \sum_{n=0}^{n_{max}} \overline{A}_n P_n(\cos\theta) \qquad (20)$$

Since the windows of the differential discriminators were adjusted so they spanned both full-energy peaks, the average energy of the two gamma rays was used to determine T. The various parameters involved in the evaluation of the integrals were the same for Channel 1 and Channel 2, therefore, $I_{n,1}$ is equal to $I_{n,2}$ and we can drop the subscript that identifies the channel. The integrals I_n for n = 0, 2, and 4 were numerically evaluated and the attenuation factors were calculated using Equation (19). The corrected angular correlation coefficients, $\overline{A}_n$, were calculated using Equation (20) and the values of A_n given in Equation (2).

The values of the parameters involved in the calculations of the corrected angular correlation coefficients are listed in Table 3.

Table 3

Solid Angle Correction Parameters

h (cm)	18.0
t (cm)	2.54
r (cm)	2.54
T (cm^{-1})	0.098
$\frac{I_2}{I_0}$	0.9870
$\frac{I_4}{I_0}$	0.9570
Q_2	0.9741
Q_4	0.9158

B. Comparison between Experiment and Theory

The experimental and corrected theoretical functions for this experiment are:

Experiment:

$$\overline{W}(\theta) = (1.0000 \pm 0.0034) + (0.0961 \pm 0.0055)\, P_2 + (0.0339 \pm 0.0071)\, P_4$$

Theoretical:

$$\overline{W}(\theta) = 1.00000 + 0.09936\, P_2 + 0.00831\, P_4$$

or, in terms of cosine functions:

Experiment:

$$\overline{W}(\theta) = (1.0000 \pm 0.0054) + (0.018 \pm 0.033) \cos^2 \theta + (0.154 \pm 0.032) \cos^4 \theta$$

Theoretical:

$$\overline{W}(\theta) = 1.0000 + 0.1236 \cos^2 \theta + 0.0381 \cos^4 \theta$$

The experimental anisotropy was calculated from the cosine function to be $\overline{R} = 0.171 \pm 0.027$ and is to be compared with $\overline{R} = 0.1617$, the theoretical anisotropy corrected for solid angle.

The corresponding correlation coefficients do not agree within statistical expectations indicating that as the equipment stands, it is not suitable for performing a precise angular correlation experiment unless the source of trouble can be located and corrected. Figure 6 is a plot of the experimental and the corrected theoretical correlation functions normalized to 90° against the angle between the directions of emission of the gamma rays. The experimental points and their standard deviations are also shown.

From Figure 6, it can be seen that the experimental points at 120° and 135° are significantly low. This could

COMPARISON BETWEEN EXPERIMENTAL AND THEORETICAL CORRELATION FUNCTIONS

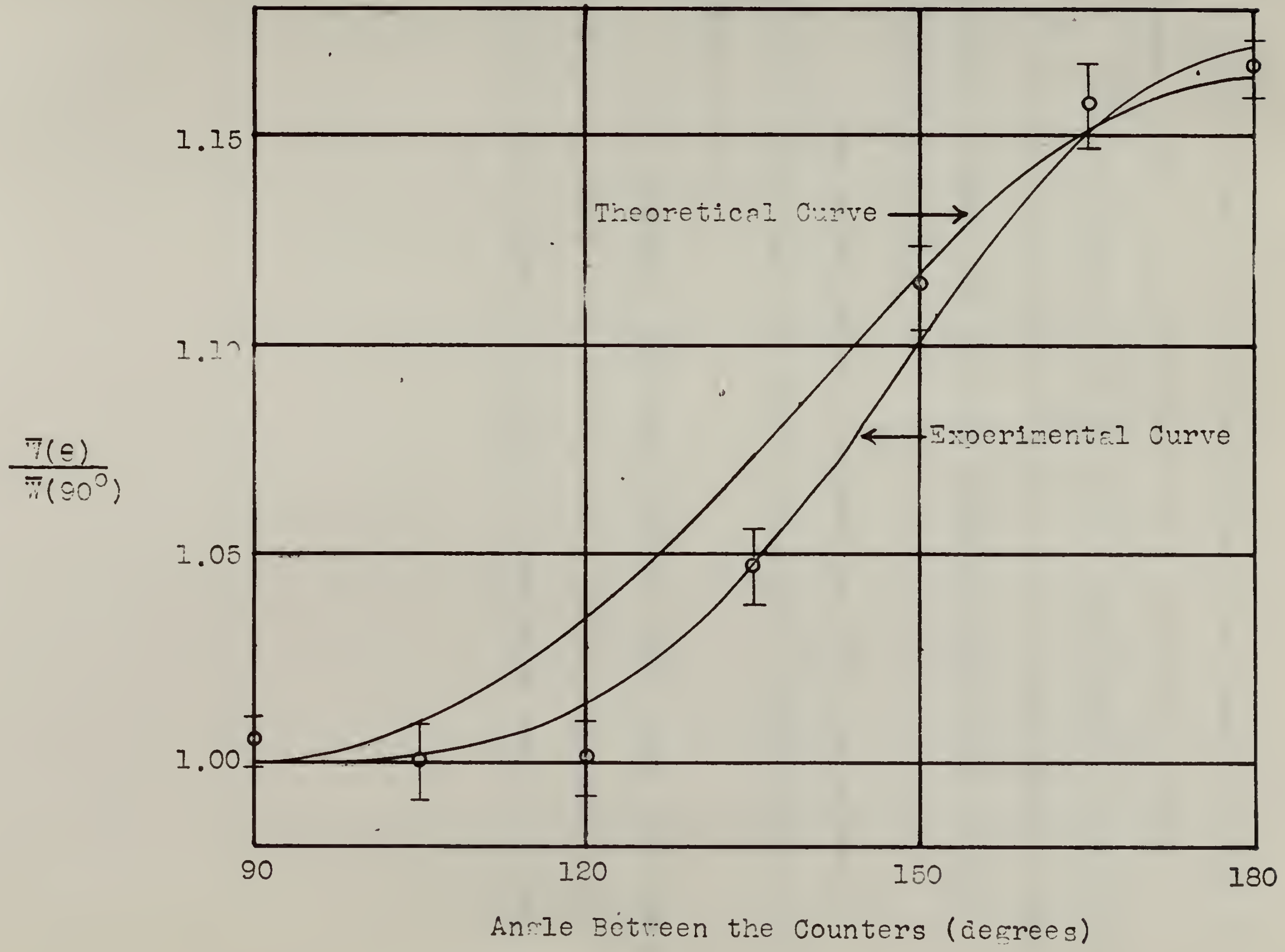

Figure 6

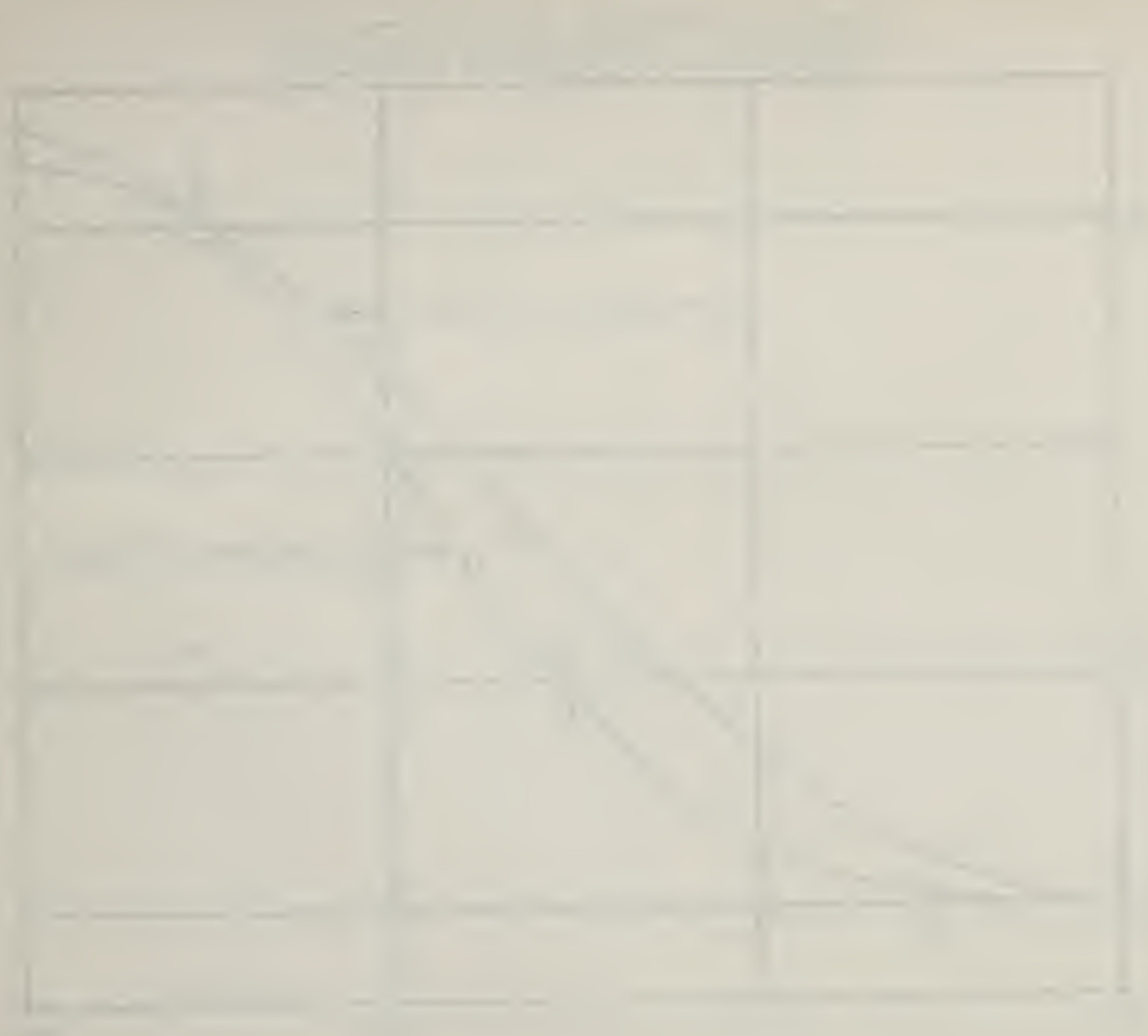

[illegible]

[illegible]

be due to statistical fluctuations, the presence of an external field, or systematic errors in the experiment.

Although this could be due to statistical fluctuations, it is quite improbable that this is the case because these points are each two or more standard deviations off the theoretical curve.

It was experimentally determined that the external field present was far smaller than that necessary to cause this effect.

It is remotely possible that the fact that the source was in a liquid form rather than a solid form could contribute to this effect, although no mechanism can be offered.

CHAPTER VII

CONCLUSIONS

As it stands, the equipment used for this experiment is not suitable for precision angular correlation investigations. Before this equipment can be used for such investigations, the reason for the distortion of the shape of the experimental correlation function discussed in Chapter VI needs to be determined and corrected. An improved coincidence analyzer whose resolving time is independent of the counting rate should be purchased or built to replace the one now in use. To provide better precision for the same counting time and source strength, the electronic system needs to be modified to reduce the accidental coincidence counting rate.

BIBLIOGRAPHY

1. D. R. Hamilton, Phys. Rev. 58, 122 (1940).
2. E. L. Brady and M. Deutsch, Phys. Rev. 72, 870 (1947).
3. L. C. Biedenharn and M. E. Rose, Rev. Mod. Phys. 25, 729 (1953).
4. M. A. Waggoner, M. L. Moon, and A. Roberts, Phys. Rev. 80, 420 (1950).
5. G. L. Keister and F. H. Schmidt, Phys. Rev. 93, 140 (1954).
6. E. D. Klema and F. K. McGowan, Phys. Rev. 91, 616 (1953).
7. M. E. Rose, Phys. Rev. 91, 610 (1953).

thesV424
Gamma-gamma angular correlation in the d
3 2768 001 92753 6
DUDLEY KNOX LIBRARY